Performance Analysis of Clustered LoRa Networks

Zhijin Qin, *Member, IEEE,* Yuanwei Liu, *Senior Member, IEEE,* Geoffrey Ye Li, *Fellow, IEEE,* and Julie A. McCann, *Member, IEEE.*

***Abstract*—In this paper, we investigate the uplink transmission performance of low-power wide-area (LPWA) networks with regards to coexisting radio modules. We adopt long range (LoRa) radio technique as an example of the network of focus even though our analysis can be easily extended to other situations. We exploit a new topology to model the network, where the node locations of LoRa follow a Poisson cluster process (PCP) while other coexisting radio modules follow a Poisson point process (PPP). Unlike most of the performance analysis based on stochastic geometry, we take noise into consideration. More specifically, two models, with a fixed and a random number of active LoRa nodes in each cluster, respectively, are considered. To obtain insights, both the exact and simple approximated expressions for coverage probability are derived. Based on them, area spectral efficiency and energy efficiency are obtained. From our analysis, we show how the performance of LPWA networks can be enhanced through adjusting the density of LoRa nodes around each LoRa receiver. Moreover, the simulation results unveil that the optimal number of active LoRa nodes in each cluster exists to maximize the area spectral efficiency.**

***Index Terms*—Low-power wide-area networks, LoRa, Poisson cluster process, stochastic geometry.**

I. Introduction

Internet of Things (IoT) is envisioned as a means to connect billions of small computing devices embedded in different environments (e.g., walls and soil) and even implanted in human bodies [2]–[5]. Aiming to provide connectivity opportunities for massive numbers of devices, two possible networking approaches have been proposed. One is the evolution from the existing communication systems, i.e., fifth generation (5G) or the beyond for intelligent communications [6], with the purpose of supporting machine-type communications (MTC) [7], [8]. Another is to design MTC-dedicated networks from scratch, such as low-power wide-area (LPWA) networks [9]–[12].

In LPWA networks, the transmission range is a dedicating factor for highly scalable smart metering or other related applications where only a small portion of data is transmitted, perhaps after considerable analysis or filtering from sensors. Another critical factor in LPWA networks is energy consumption since they consist of energy-constrained devices. The battery lifetime of some smart city sensors is required to be no less than ten years for IoT applications [13]. Two technical options have been proposed for LPWA networks to enhance signal-to-noise ratio (SNR) ratio and to increase transmission ranges with enhanced power efficiency; they are the ultra narrrowband approach and the coding gain approach. The ultra narrowband approach enhances SNR by focusing signal in a narrowband. One of the classic technologies, Sigfox [14] uses the narrowband approach to implement an LPWA network. The other approach exploits coding gain to combat high noise power in a wideband receiver. Long range (LoRa) radio technique [15] is an example of the code gain approach.

LoRa has a relatively long transmission range and low energy consumption, which has attracted much attention in IoT field and became the most widely deployed LPWA technique. Furthermore, the chirp spread spectrum technology used in LoRa allows the usage of cheap oscillators with high stability guaranteed at the receiver [15]. These advantages make LoRa a popular candidate for smart city scenarios. LoRaWAN is a medium access control (MAC) protocol for LoRa, and supports star-topologies providing high capacity and longer transmission ranges [15]. The uplink of LoRaWAN is scheduled by end-devices based on their transmission requirements, regardless of the channel occupancy. LoRaWAN achieves low energy consumption since it does not sense the medium before sending its packet and does not require any synchronization to access the medium. However, packet collision remains a problem. The coverage probability of LoRa networks has been analyzed [16] by considering the interfering signals using the same spreading factor (SF). However, we believe that both intra-interference, i.e., from LoRa users in the same and neighbouring networks, and inter-interference, i.e., from other LPWA users sharing the same spectrum, combat the performance of LPWA networks [1]. So far, some experiments on LoRa and other LPWA techniques have been carried out as the initial trials in wireless sensor networks [12], [17]–[21]. Particularly, we have deployed LoRa devices in the Queen Elizabeth Park, London, to collect data and installed a LoRa gateway to forward the collected data to a cloud server for further processing and analyzing [12]. Based on this implementation, we have further investigated the resource efficiency and energy efficiency in LoRa networks by optimizing the channel selection and transmit power of LoRa users [22], [23].

To make this work more general, we theoretically analyze the performance of clustered LPWA networks with particular focus on the interference from coexisting LoRa users and other LPWA users, as they all work over unlicensed spectrum. Stochastic geometry is a powerful mathematical tool for designing and analyzing wireless networks, particularly dense networks [24], such as LPWA networks that potentially provide massive connectivity. When wireless nodes are uniformly distributed in an area, homogeneous Poisson

Part of the work has been presented in IEEE International Conference on Communications, Paris, France, May, 2017 [1]. This work was funded by ICRI.

Zhijin Qin and Yuanwei Liu are with Queen Mary University of London, London E1 4NS, UK, (e-mail: {z.qin; yuanwei.liu}@qmul.ac.uk). Zhijin Qin is also with Imperial College London as an Honorary Research Fellow.

Geoffrey Ye Li is with Georgia Institute of Technology, Atlanta, GA, USA, 30332-0250 (e-mail: liye@ece.gatech.edu).

Julie A. McCann is with Imperial College London, London SW7 2AZ, UK, (email: j.mccann@imperial.ac.uk).

point processes (PPPs) can accurately model dense networks. However, when sensors are clustered, such as in smart city scenarios, PPP is unable to model interference [25]. In this situation, Poisson cluster process (PCP), where parent points form a PPP and offspring points form clusters centred at the parent point, is necessary to model wireless networks using random cluster topologies arising from geographical factors or MAC protocols [25], [26].

PCPs have attracted lots of attention in cellular networks and wireless sensor networks [27]–[33], recently. In [27], an interference alignment approach has been used for a cluster topology to address intra-cluster interference for multiple-input multiple-output (MIMO) systems, where a spatial PCP process is used to model the nodes in a random access network. For heterogeneous cellular networks, PCP has been adopted in [28], [29] to model nodes clustering at hot spots while taking into consideration the fact that base stations belonging to different tiers may differ in terms of transmit power, node density, and link reliability. In [30], the PCP model has been applied to wirelessly powered backscatter communications, where power beacons (PBs) form the parent PPP and the backscatter nodes are children points in the cluster. A *Thomas* PCP model can capture the fact that a given device typically has multiple proximate devices, any of which can potentially act as a serving device. It has been used to model the device locations for device-to-device (D2D) networks in [31]. Moreover, a *Matern* PCP has been used to model wireless networks exhibiting device clustering and the distance distribution has been derived to describe the interference statistics and connection probability in clustered networks [32]. Based on the results, the *Matern* PCP and modified Thomas PCP have been investigated when they are adopted to model the out-of-band D2D networks [33]. Furthermore, it has been pointed out that clustering is beneficial for long range transmissions in ad-hoc networks [25]. Therefore, the PCP can model LPWA networks well.

While the aforementioned research contributions have laid a solid foundation and provided a good understanding on the PCP model, the performance analysis using PPP/PCP based stochastic geometry approach to investigate LPWA networks is still missing. Different from the clustered D2D networks, LoRa works over unlicensed spectrum, which makes the network suffering from the most severe interference caused by: i) The LoRa nodes in the same cluster, which is due to the non-orthogonality of SFs; ii). The LoRa nodes clustered in the neighbouring clusters accessing the same channel; iii). The non-LoRa nodes that are using other radio access networks over the same unlicensed channel. In this paper, we adopt *Matern* cluster process [34] to model LPWA networks, where the LoRa receivers forms PPP cluster centers and the active LoRa nodes in each cluster form the children process since sensor nodes, like metering sensors distributed in a building, are highly clustered based on geography. We also assume that the coexisting non-LoRa nodes are modelled as PPP. This topology is motivated by the fact that we can only control the clustering deployment of LoRa nodes rather than non-LoRa ones. Therefore, non-LoRa nodes may use any coexisting radio and locate at any location within the considered area. Moreover, unlike existing research that mostly considers the interference-limited case, we additionally consider the impact of noise on the system performance. The reason is that LPWA networks are not necessary interference-limited due to the long transmission distance with relatively low transmit power.

To the best of our knowledge, this work is the first attempt to model and analyze LPWA networks using the *Matern* PCP model. In this paper, we attempt to explore the potential performance enhancement brought by PCP as well as to answer the following questions:

1) What is the impact in terms of the cluster radius on the system performance?
2) Is there an optimal number of active LoRa nodes in each cluster?
3) What is the most appropriate transmit power for LoRa users?

The major contributions of this paper are summarized as follows:

1) We use the spatial distributions of PCP to model the LoRa system by considering the potential interference from both co-existing LoRa users and non-LoRa users working over the same channel. Specifically, By considering the uplink transmission of LoRa networks, the *Marten* cluster process is invoked to model the locations of LoRa nodes as well as receivers. Moreover, the PPP model is adopted to model non-LoRa nodes communicating over the same channel as the LoRa users.
2) To characterize the performance of the LPWA networks, three performance metrics, including coverage probability, area spectral efficiency, and energy efficiency, are adopted. By using Gaussian-Chebyshev approximation, we derive both exact and simple approximated expressions of these three metrics with considering the impact of channel noise.
3) We analytically prove that significant performance gains can be achieved by decreasing the radius of each cluster. We also demonstrate that there exists an optimal number of active LoRa nodes for each cluster that can maximize the area spectral efficiency. These remarks provide insightful guidelines for the implementation of LPWA networks.

The rest of the paper is organized as follows. In Section II, the system model for LPWA networks with LoRa is introduced. In Section III, new analytical expressions for the coverage probability of the considered networks are derived. Then area spectral efficiency and energy efficiency are investigated in Section IV. Numerical results are presented in Section V, which is followed by the conclusions in Section VI.

II. System Model

In this section, the system settings and propagation model are introduced for the considered LoRa LPWA networks and other coexisting LPWA radio modules that work over the same frequency.

A. Spatial Setup and Key Assumptions

We consider the uplink transmission in LPWA networks where the system under study is LoRa with interference from

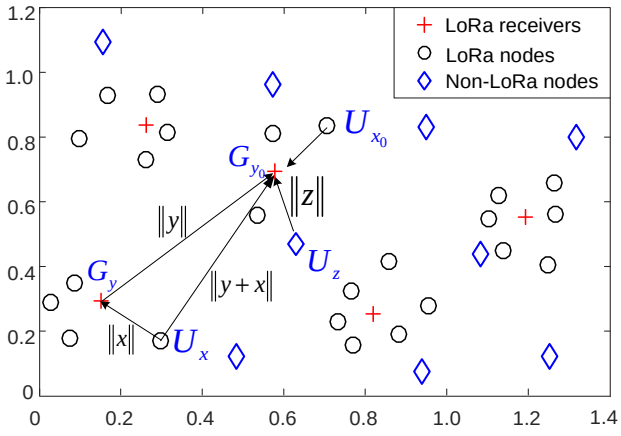

Fig. 1. System model of the clustered low-power wide-area networks with LoRa and coexisting radios.

other LPWA radio modules (e.g., Sigfox). A star-topology is adopted and the nodes use single-hop wireless communications to gateways [15]. As shown in Fig. 1, the locations of all LoRa nodes are modeled by a PCP, where the LoRa receivers follow the parent point process and the offspring point process (one per parent) are conditionally independent. Specifically, the locations of the LoRa receivers are modeled as a PPP, Φ_G, with density λ_G. In each cluster, the locations of the LoRa nodes served by the parent receiver are conditionally independent. The union of all the offspring LoRa nodes constitute a PCP, namely, a *Matern* cluster process. In this LoRa network, we consider two models for the number of active LoRa nodes distributed in each cluster. One is that the number of active LoRa nodes in each cluster is fixed as n. Another is that the number of active LoRa nodes is random and follows a Poisson distribution with average $\bar{n}$. Different LoRa nodes communicate with the same receiver over the same channel simultaneously by adopting different SFs. Different SFs will lead to different transmission ranges and data rates, for instance, SF 7 can achieve the highest data rate while the transmission distance is limited compared to SF 12.[1]

As in many practical environments, we also assume that there exist non-LoRa nodes transmitting on the same channel, which refer to nodes connecting to other non-LoRa radio modules, as LoRa is working on the unlicensed spectrum. Those nodes are modeled as a PPP, $\Phi_{\rm co}$, with density $\lambda_{\rm co}$, labeled by diamonds in Fig. 1, shows coexistence interference at the LoRa receiver. In a network with LoRa modules only, coexistence interference becomes zero by tuning the density of the non-LoRa nodes as $\lambda_{\rm co} = 0$.

B. Propagation Model

As shown in Fig. 1, for a typical LoRa node, U_{x_0}, the signal-to-interference-plus-noise ratio (SINR) received at a typical LoRa receiver, G_{y_0}, can be expressed as

$$SINR = \frac{P_{x_0} h_{x_0,y_0} L(R)}{I_{\rm intra} + I_{\rm inter} + I_{\rm co} + \sigma^2}, \tag{1}$$

[1]How to allocate SFs among different users is out the scope of this paper.

where $I_{\rm intra}$, $I_{\rm inter}$, and $I_{\rm co}$ refer to the average powers of intra-interference caused by the non-orthogonality of SFs adopted by LoRa nodes within the same cluster, inter-cluster interference caused by LoRa nodes in the neighboring clusters, and coexistence interference from nodes connecting to non-LoRa radio modules, respectively. These interferences are independent since they are from different sources, and σ^2 is the power of additive white Gaussian noise (AWGN), and P_{x_0} refers to the transmit power from the typical LoRa node, U_{x_0}, and $h_{x_0,y_0} \sim \exp(1)$ and $L(R)$ refer to small-scale fading coefficient and large-scale fading coefficient between the desired LoRa node and its receiver, G_{y_0}, respectively. In (1), $L(R) = \eta \|x_0\|^{-\alpha}$, where η is a frequency dependent factor, $\|x_0\|$ is the distance between the desired LoRa node and its receiver, and α is the path loss exponent.

To get an analytical expression of SINR, we will find $I_{\rm intra}$, $I_{\rm inter}$, and $I_{\rm co}$ subsequently.

1) Intra-cluster interference: At G_{y_0}, interference from LoRa nodes within the same cluster except the typical one is

$$I_{\rm intra} = \sum_{x \in N_{y_0} \setminus x_0} P_x h_{x,y_0} \eta \|x\|^{-\alpha}, \tag{2}$$

where P_x refers to the transmit power of the interference LoRa nodes within the same cluster, and $h_{x,y_0} \sim \exp(1)$ is the small-scale fading coefficient, and $\|x\|$ is the distance between LoRa node and the LoRa receiver in the same cluster, as shown in Fig. 1. Here, N_{y_0} is the number of the active LoRa nodes that simultaneously transmit to the same receiver, G_{y_0}, within a cluster, which is n for the fixed number of active LoRa nodes model and follows a Poisson distribution with average $\bar{n}$ for the random model.

2) Inter-cluster interference: The interference from LoRa nodes in the adjacent clusters is

$$I_{\rm inter} = \sum_{y \in \Phi_G \setminus y_0} \sum_{x \in N_y} P_x h_{x,y} \eta \|y + x\|^{-\alpha}, \tag{3}$$

where P_x is the transmit power from the LoRa nodes served by the neighboring LoRa receiver, G_y, and $h_{x,y} \sim \exp(1)$ is the small-scale fading coefficient, and $\|y + x\|$ refers to the distance between the LoRa node, U_x, which is served by the neighboring LoRa receivers, G_y, and the typical LoRa receiver, G_{y_0}, as shown in Fig. 1. N_y is the number of active LoRa nodes served by the LoRa receiver, G_y, in the same cluster.

3) Coexistence interference: We also consider interference from non-LoRa nodes transmitting over the same frequency, which follows a PPP, $\Phi_{\rm co}$, with a density $\lambda_{\rm co}$. As such, the interference from these nodes can be expressed as

$$I_{\rm co} = \sum_{z \in \Phi_{\rm co}} P_z h_{z,y_0} \eta \|z\|^{-\alpha}, \tag{4}$$

where P_z is the transmit power from the non-LoRa node, U_z, served by non-LoRa radio modules, the distance between the LoRa node, U_z, and the typical LoRa receiver, G_{y_0}, is $\|z\|$, and $h_{z,y_0} \sim \exp(1)$ is small-scale fading coefficient, as shown in Fig. 1.

III. Interference Analysis

In this section, we analyze the intra interference, inter interference and coexistence interference for the models with a fixed and a random number of LoRa nodes in each cluster, where we consider both the ordered case and unordered case. The *unordered case* refers to that the typical LoRa node in the typical cluster is chosen randomly from the set of active LoRa nodes in one cluster. The *ordered case* refers to that the typical LoRa node is located at the k-th closest distance to the LoRa receiver among the active nodes in one cluster. Therefore, there are four scenarios. In this section, we are going to investigate the interference for the four scenarios, respectively.

A. Distance Distributions

1) Unordered distance PDF for intra-cluster: For a *Matern* cluster process, the probability density function (PDF) of the distance, r, between a typical receiver centered at a cluster and a connected LoRa node is [25]

$$f_{\|x\|}(x) = \begin{cases} \frac{1}{\pi a^2}, \ \|x\| \leq a. \\ 0, \text{otherwise}, \end{cases} \tag{5}$$

where a is the cluster radius. When converting (5) to polar coordinates, we have

$$f_R(r) = \begin{cases} \frac{2r}{a^2}, r \leq a. \\ 0, \text{otherwise}. \end{cases} \tag{6}$$

2) Ordered distance PDF for intra-cluster: In the ordered case, the PDF for intra-cluster can be given by the following lemma.

Lemma 1. *If n_ι active LoRa nodes are uniformly distributed within a cluster with radius, a, then the PDF of the distance of the k-th closest LoRa node connecting to the typical LoRa receiver is given by*

$$f_{\tilde{r}_k}(r) = \begin{cases} \frac{2n_\iota! \sum_{p=0}^{n_\iota - k} (-1)^p a^{-2(p+k)} r^{2(p+k)-1}}{(n_\iota - k)!(k-1)!}, r \leq a. \\ 0, \ \text{otherwise}, \end{cases} \tag{7}$$

where $n_\iota \in \{n, \bar{n}\}$.

Proof. With the aid of order statistics [35], the ordered distance PDF is given by

$$f_{\tilde{r}_k}(r) = \frac{n_\iota! (F_R(r))^{k-1} (1 - F_R(r))^{n_\iota - k} f_R(r)}{(n_\iota - k)!\,(k-1)!}, \tag{8}$$

where

$$F_R(r) = \frac{r^2}{a^2} \tag{9}$$

is the CDF of the unordered intra-cluster distance. Substituting $F_R(r)$ and (6) into (8) and applying binomial series expansion, we can obtain (7). The proof is completed. □

3) PDF of the ordered distance for intra-cluster interference LoRa nodes: Since we are interested in the performance of the k-th closest LoRa node, its corresponding intra-cluster interference nodes are dependent on the distance rank k. To better incorporate our analytical procedure, besides the k-th LoRa node, we further divide the rest $(n_\iota - 1)$ nodes into two sets. Those closer than the k-th one, $\mathcal{K}_{near} = \{1, \cdots, k-1\}$, and those farther away than the k-th one, $\mathcal{K}_{far} = \{k+1, \cdots, n_\iota\}$.

Lemma 2. *The PDF of the ordered LoRa nodes that interfere the k-th closest node in the same cluster is given by*

$$f_{\tilde{R}}(r|\,\tilde{r}_k) = \begin{cases} \frac{2r}{\tilde{r}_k^2}, r \leq \tilde{r}_k. \\ \frac{2r}{a^2 - \tilde{r}_k^2}, \tilde{r}_k < r \leq a, \end{cases} \tag{10}$$

where $\tilde{r}_k$ denotes the distance from the k-th closest LoRa node to the serving receiver.

Proof. Following the same procedure for obtaining Lemma 4 in [31], with the aid of ordered statistics (7) and applying the symmetry property, we can obtain the distance PDF of the ordered intra-cluster for $\mathcal{K}_{near}$ and $\mathcal{K}_{far}$ as $f_{r_{near}}(r_{near}|\,\tilde{r}_k) = \frac{f_R(r_{near})}{F_R(\tilde{r}_k)}$ and $f_{r_{far}}(r_{far}|\,\tilde{r}_k) = \frac{f_R(r_{far})}{1 - F_R(\tilde{r}_k)}$, respectively. Then with the aid of (8) and (9), we can obtain the desired result in (10). The proof is completed. □

B. Laplace Transforms for Interferences of Unordered LoRa Nodes

In the following, we turn our attention to obtaining the Laplace transforms of the interference parts for the unordered cases with a fixed and a random number of active LoRa nodes in each cluster, respectively.

1) Intra-cluster interference: We first address the intra-cluster interference.

Lemma 3. *For the unordered case with a fixed number of active nodes n in each cluster, the Laplace transform of intra-cluster interference can be expressed as*

$$\mathcal{L}_{I^n_{\text{intra}}}(s) = \left[\frac{a^\alpha \delta}{sP_x \eta (\delta + 1)} {}_2F_1\left(1, \delta + 1; \delta + 2; -\frac{a^\alpha}{sP_x \eta}\right) \right]^{n-1}, \tag{11}$$

and for the unordered case with with a random number of active LoRa nodes of average $\bar{n}$ in the cluster, the Laplace transform of intra-cluster interference can be expressed as

$$\mathcal{L}_{I^{\bar{n}}_{\text{intra}}}(s) = \exp\left(-(\bar{n} - 1) {}_2F_1\left(1, \delta; \delta + 1; -\frac{a^\alpha}{sP_x \eta}\right) \right), \tag{12}$$

where ${}_2F_1(\,)$ is the is the Gauss hypergeometric function.

Proof. See Appendix A. □

To obtain more insightful and simple expressions, we use Gauss-Chebyshev approximation, which is regarded as a tight approximation and has been widely used [36]–[40], to approximate (11) and (12). It is shown by the following corollary.

Corollary 1. *For the unordered case with a fixed number of active LoRa nodes in the cluster, the Laplace transform of the intra-cluster interference can be approximated as*

$$\mathcal{L}^{ap}_{I^{n}_{\text{intra}}}(s) \approx \left[\omega_T \sum_{t=1}^{T} \frac{\mu_t c_t^{\alpha+1}}{c_t^{\alpha} + a^{-\alpha} s P_x \eta}\right]^{n-1}, \tag{13}$$

and for the unordered case with a random number of active LoRa nodes with average $\bar{n}$ in the cluster, the Laplace transform of the intra-cluster interference can be approximated as

$$\mathcal{L}_{I^{\bar{n},ap}_{\text{intra}}}(s) \approx \exp\left(-(\bar{n}-1)\,\omega_T \sum_{t=1}^{T} \frac{\mu_t c_t}{\frac{c_t^{\alpha} a^{\alpha}}{s P_x \eta} + 1}\right), \tag{14}$$

where $\omega_T = \frac{\pi}{T}, \psi_t = \cos\left(\frac{2t-1}{2T}\pi\right), c_t = \frac{(\psi_t+1)}{2}$, and $\mu_t = \sqrt{1-\psi_t^2}$.

2) Inter-cluster interference: Here, we provide the Laplace transforms of the inter-cluster interference for a fixed and a random number of active LoRa nodes in the cluster, respectively.

Lemma 4. *The Laplace transform of the inter-cluster interference with a fixed number of active nodes n in the cluster is upper bounded by*

$$L^{up}_{I^{n}_{\text{inter}}}(s) = \tag{15}$$
$$exp\left(-\pi\lambda_G (s P_x \eta)^{\delta} \delta \sum_{p=1}^{n} \binom{n}{p} B(p-\delta, n-p+\delta)\right),$$

where $B(\cdot,\cdot)$ is the Beta function. Here, $B(x,y) = \int_0^{\infty} \frac{t^{x-1}}{(1+t)^{x+y}} dt$ for $x, y > 0$.

The Laplace transform of the inter-cluster interference with a random number of active nodes of average $\bar{n}$ in a cluster is lower bounded by

$$\mathcal{L}^{low}_{I^{\bar{n}}_{\text{inter}}}(s) = \exp\left(-\pi^2 \lambda_G \bar{n} (s P_x \eta)^{\delta} \frac{\delta}{\sin(\pi\delta)}\right). \tag{16}$$

Proof. For the proof of (15), see Appendix B. For the proof of (16), see Appendix C. □

3) Coexistence interference: For coexistence interference, we can obtain the following lemma.

Lemma 5. *The Laplace transform of coexistence interference, which comes from the nodes connecting to non-LoRa radio modules, can be expressed as*

$$\mathcal{L}_{I_{\text{co}}}(s) = \exp\left(-\pi\lambda_{\text{co}}\Gamma(1+\delta)\Gamma(1-\delta)(s P_z \eta)^{\delta}\right), \tag{17}$$

where $\delta = \frac{2}{\alpha}$.

Proof.

$$\begin{aligned}\mathcal{L}_{I_{\text{co}}}(s) &= \mathbb{E}_{I_{\text{co}}}\left\{\exp\left(-s \sum_{z\in\Phi_{\text{co}}} P_z h_{z,y_0} \eta \|z\|^{-\alpha}\right)\right\} \\ &\overset{(a)}{=} \mathbb{E}_{\Phi_{\text{co}}}\left\{\prod_{z\in\Phi_{\text{co}}} \mathbb{E}_{h_{z,y_0}}\left[\exp\left(-s P_z h_{z,y_0}\eta\|z\|^{-\alpha}\right)\right]\right\} \\ &\overset{(b)}{=} \exp\left(-2\pi\lambda_{\text{co}} \int_0^{\infty}\left(1 - \frac{1}{1+s P_z \eta r^{-\alpha}}\right) r dr\right),\end{aligned} \tag{18}$$

where (a) is obtained by applying the generating function, and (b) is obtained by the fact that g_{z,y_0} follows a Rayleigh fading distribution. By applying [41, Eq. (3.241) .4], we can obtain (17). The proof is completed. □

C. Laplace Transforms for Interferences of Ordered LoRa Users

Lemma 6. *For the ordered case with a fixed number of active nodes n in the cluster, the Laplace transform of intra-cluster interference can be expressed as*

$$\mathcal{L}_{I^{n,k}_{\text{intra}}}(s) = \left[\frac{\tilde{r}_k^{\alpha}\delta}{s P_x \eta(\delta+1)} Z_1(\tilde{r}_k)\right]^{k-1} \tag{19}$$
$$\left[\frac{\delta}{(a^2 - \tilde{r}_k^2) s P_x \eta(\delta+1)}\left(a^{\alpha+2} Z_1(a) - \tilde{r}_k^{\alpha+2} Z_1(\tilde{r}_k)\right)\right]^{n-k},$$

where

$$Z_1(\tilde{r}_k) = {}_2F_1\left(1, \delta+1; \delta+2; -(s P_x \eta)^{-1} \tilde{r}_k^{\alpha}\right), \tag{20}$$

and

$$Z_1(a) = {}_2F_1\left(1, \delta+1; \delta+2; -(s P_x \eta)^{-1} a^{\alpha}\right). \tag{21}$$

For the ordered case with a random number of active LoRa nodes in the cluster, with the number of active LoRa users, $\mathcal{N}$, no fewer than the average number, $\bar{n}$, the corresponding Laplace transform of intra-cluster interference can be expressed as

$$\mathcal{L}_{I^{\bar{n},\mathcal{N}}_{\text{intra}}}(s) = \exp\left[-(\bar{n}-1)\,{}_2F_1\left(1, \delta; \delta+1; -(s P_x \eta)^{-1} \tilde{r}_{\mathcal{N}}^{\alpha}\right)\right], \tag{22}$$

where $\tilde{r}_{\mathcal{N}}$ is the distance from the LoRa node to the serving receiver.

Proof. For the proof, see Appendix D. □

From Lemma 6 and using Gauss-Chebyshev approximation, we can obtain the following corollary.

Corollary 2. *For the ordered case with a fixed number of active LoRa nodes n in the cluster , the Laplace transform of intra-cluster interference can be approximated as*

$$\mathcal{L}^{ap}_{I^{n,k}_{\text{intra}}}(s) \approx \left[\omega_T \sum_{t=1}^{T} \frac{\mu_t c_t^{\alpha+1}}{c_t^{\alpha} + \tilde{r}_k^{-\alpha} s P_x \eta}\right]^{k-1} \times \tag{23}$$
$$\left[\frac{\omega_T}{a^2 - \tilde{r}_k^2}\left(a^2 \sum_{t=1}^{T} \frac{\mu_t c_t^{\alpha+1}}{c_t^{\alpha} + a^{-\alpha} s P_x \eta} - \tilde{r}_k^2 \sum_{t=1}^{T} \frac{\mu_t c_t^{\alpha+1}}{c_t^{\alpha} + \tilde{r}_k^{-\alpha} s P_x \eta}\right)\right]^{n-k},$$

and for the ordered case with a random number of active LoRa nodes with average $\bar{n}$ in the cluster, the Laplace transform of intra-cluster interference can be approximated as

$$\mathcal{L}^{ap}_{I^{\bar{n},\mathcal{N}}_{\text{intra}}}(s) \approx \exp\left(-(\bar{n}-1)\,\omega_T \sum_{t=1}^{T} \frac{\mu_t c_t}{\frac{c_t^{\alpha}\tilde{r}_{\mathcal{N}}^{\alpha}}{s P_x \eta} + 1}\right). \tag{24}$$

Note that the Laplace transforms of inter-cluster interference and coexistence interference for the ordered case are the same as those in the unordered case, which are given in the last subsection.

IV. Coverage Probability Analysis

In this section, we derive the coverage probability for a typical LoRa node based on the interference analysis in the previous section. The coverage probability is defined as the probability that a typical user can be successfully decoded at the receiver, that is SINR of the typical user received at the receiver is higher than a threshold, γ_{th}. It can be expressed as

$$P_{\rm cov}\left(\gamma_{th}\right) = \mathbb{E}_R\left[\Pr\left\{\mathrm{SINR}\left(R\right) \geq \gamma_{th}\right\} | \, R\right], \tag{25}$$

where R is the distance between the desired LoRa node and the serving receiver in the same cluster.

By applying (1) and (5) into (25), the transmission coverage probability of a typical LoRa node can be expressed as

$$P_{\rm cov}\left(\gamma_{th}\right) = \int \Pr\left\{\mathrm{SINR}\left(R\right) \geq \gamma_{th}\right\} f_R\left(r\right) dr. \tag{26}$$

From (25), we can obtain

$$\begin{aligned}
&\Pr\left\{\mathrm{SINR}\left(R\right) \geq \gamma_{th}\right\} = \Pr\left\{\frac{P_{x_0} h_{x_0,y_0} L\left(R\right)}{I_{\rm intra} + I_{\rm inter} + I_{\rm co} + \sigma^2} \geq \gamma_{th}\right\} \\
&= \Pr\left\{h_{x_0,y_0} \geq \left(I_{\rm intra} + I_{\rm inter} + I_{co} + \sigma^2\right) \frac{\eta R^{\alpha} \gamma_{th}}{P_{x_0}}\right\} \\
&= e^{-\rho\sigma^2} \mathbb{E}_{I_{\rm intra}+I_{\rm inter}+I_{\rm co}}\left\{e^{-\rho\left(I_{\rm intra}+I_{\rm inter}+I_{\rm co}\right)}\right\} \\
&= e^{-\rho\sigma^2} \mathcal{L}_{I_{\rm intra}}\left(\rho\right) \mathcal{L}_{I_{\rm inter}}\left(\rho\right) \mathcal{L}_{I_{\rm co}}\left(\rho\right),
\end{aligned} \tag{27}$$

where $\rho = \frac{R^{\alpha}\gamma_{th}}{P_{x_0}\eta}$, $\mathcal{L}_{I_{\rm intra}}\left(\rho\right) = \mathbb{E}\left\{e^{-\rho I_{\rm intra}}\right\}$, $\mathcal{L}_{I_{\rm inter}}\left(\rho\right) = \mathbb{E}\left\{e^{-\rho I_{\rm inter}}\right\}$, and $\mathcal{L}_{I_{\rm co}}\left(\rho\right) = \mathbb{E}\left\{e^{-\rho I_{\rm co}}\right\}$ are the Laplace transforms of the power density distributions of $I_{\rm intra}$, $I_{\rm inter}$ and $I_{\rm co}$, respectively.

A. Coverage Probability of Unordered LoRa Users

Based on the derived results in Section III, we can obtain the coverage probability of a typical LoRa node for the unordered case in this subsection.

Theorem 1. *If the LoRa nodes follow a Matern cluster process centered around each receiver, for the unordered case with a fixed number of LoRa nodes in the cluster, the upper bound of the coverage probability of a typical LoRa node can be expressed as*

$$P^{n}_{\rm cov,up}\left(\gamma_{th}\right) = \frac{2}{a^2}\int_0^a e^{-\rho\sigma^2} \mathcal{L}_{I^{n}_{\rm intra}}\left(\rho\right) \mathcal{L}^{up}_{I^{n}_{\rm inter}}\left(\rho\right) \mathcal{L}_{I_{\rm co}}\left(\rho\right) r dr, \tag{28}$$

where $\mathcal{L}_{I^{n}_{\rm intra}}\left(\rho\right)$, $\mathcal{L}^{up}_{I^{n}_{\rm inter}}\left(\rho\right)$, and $\mathcal{L}_{I_{\rm co}}\left(\rho\right)$ are given by (11)*,* (15)*, and* (17)*.*

For the unordered case with a random number of LoRa nodes in the cluster with average $\bar{n}$, the lower bound of the coverage probability of a typical LoRa node can be expressed as

$$P^{\bar{n}}_{\rm cov,low}\left(\gamma_{th}\right) = \frac{2}{a^2}\int_0^a e^{-\rho\sigma^2} \mathcal{L}_{I^{\bar{n}}_{\rm intra}}\left(\rho\right) \mathcal{L}^{low}_{I^{\bar{n}}_{\rm inter}}\left(\rho\right) \mathcal{L}_{I_{\rm co}}\left(\rho\right) r dr, \tag{29}$$

where $\mathcal{L}_{I^{\bar{n}}_{\rm intra}}\left(\rho\right)$, $\mathcal{L}^{low}_{I^{\bar{n}}_{\rm inter}}\left(\rho\right)$, and $\mathcal{L}_{I_{\rm co}}\left(\rho\right)$ are given by (12)*,* (16)*, and* (17)*.*

Proof. Substituting (6) and (27) into (26), and basing the derived results of Lemmas 3, 4 and 5, we can obtain the desired result in (28). The proof procedure of obtaining (29) is similar to the above for (28), and is hence skipped here. □

Note that it is hard to see insights directly from (28) and (29). To obtain more insightful expressions, we derive the following corollary.

Corollary 3. *If the LoRa nodes follow a Matern cluster process centered around each receiver, for the unordered case with a fixed number of LoRa nodes in the cluster, the coverage probability of a typical LoRa node can be approximated as*

$$\begin{aligned}
&P^{n,ap}_{\rm cov,up}\left(\gamma_{th}\right) \approx \\
&\omega_M \sum_{m=1}^{M} \vartheta_m l_m \exp\left(-\rho_m \sigma^2\right) \left[\omega_T \sum_{t=1}^{T} \frac{\mu_t c_t^{\alpha+1}}{c_t^{\alpha} + \gamma_{th}\tilde{P}_x^{-1}}\right]^{n-1} \\
&\exp\left[-a^2 l_m^2 \pi \lambda_G \delta \sum_{p=1}^{n} \binom{n}{p} B\left(p-\delta, n-p+\delta\right) \left(\gamma_{th}\tilde{P}_x^{-1}\right)^{\delta}\right] \\
&\exp\left[-\frac{a^2 l_m^2 \pi^2 \delta}{\sin\left(\pi\delta\right)} \lambda_{\rm co} \left(\gamma_{th}\tilde{P}_z^{-1}\right)^{\delta}\right],
\end{aligned} \tag{30}$$

where $\tilde{P}_x = \frac{P_{x_0}}{P_x}$, $\tilde{P}_z = \frac{P_{x_0}}{P_z}$, $\omega_M = \frac{\pi}{M}$, $\nu_m = \cos\left(\frac{2m-1}{2M}\pi\right)$, $l_m = \frac{(\nu_m+1)}{2}$, $\rho_m = \frac{l_m^{\alpha} a^{\tilde{\alpha}} \gamma_{th}}{P_{x_0}\eta}$, and $\vartheta_m = \sqrt{1-\nu_m^2}$, $\omega_T = \frac{\pi}{T}$, $\psi_t = \cos\left(\frac{2t-1}{2T}\pi\right)$, $c_t = \frac{(\psi_t+1)}{2}$, and $\mu_t = \sqrt{1-\psi_t^2}$.

For the unordered case with a random number of active LoRa nodes in the cluster with average $\bar{n}$, the coverage probability of a typical LoRa node can be approximated as

$$\begin{aligned}
&P^{\bar{n},ap}_{\rm cov,low}\left(\gamma_{th}\right) \approx \omega_M \sum_{m=1}^{M} \vartheta_m l_m \exp\left\{-\rho_m\sigma^2 - \left(\bar{n}-1\right)\omega_T\right. \\
&\left.\sum_{t=1}^{T} \frac{\mu_t c_t}{\frac{c_t^{\alpha}\tilde{P}_x}{l_m^{\alpha}\gamma_{th}} + 1} - \frac{a^2 l_m^2 \pi^2 \delta}{\sin\left(\pi\delta\right)} \left(\lambda_G \bar{n} \left(\frac{\gamma_{th}}{\tilde{P}_x}\right)^{\delta} + \lambda_{\rm co}\left(\frac{\gamma_{th}}{\tilde{P}_z}\right)^{\delta}\right)\right\}.
\end{aligned} \tag{31}$$

Proof. For simplicity, by using the approximated expressions of the Laplace transform rather than the exact expressions, we can obtain

$$P^{n,ap}_{\rm cov,up}\left(\gamma_{th}\right) \approx \frac{2}{a^2}\int_0^a e^{-\rho\sigma^2} \mathcal{L}^{ap}_{I^{n}_{\rm intra}}\left(\rho\right) \mathcal{L}^{up}_{I^{n}_{\rm inter}}\left(\rho\right) \mathcal{L}_{I_{\rm co}}\left(\rho\right) r dr. \tag{32}$$

Then based on the derived results of Corollary 1, Lemmas 4 and 5, with the aid of Gauss-Chebyshev approximation, we can obtain the desired results in closed-form as (30). The proof procedure to obtain (31) is similar to the above for (30), and is hence skipped here. □

Remark 1. *The coverage probability is a monotonic decreasing function of $n_{\iota} \in \{n, \bar{n}\}$, λ_G, and $\lambda_{\rm co}$. This indicates that increasing the average number of LoRa nodes that simultaneously transmit to the same LoRa receiver degrades the coverage probability. It is further observed that one either increases the density of active LoRa nodes, or the density of active non-LoRa nodes degrades the coverage probability, as more intra-interference and inter-interference are introduced.*

Remark 2. *The coverage probability is a monotonic decreasing function of the cluster radius, a. Hence, if the LoRa nodes are densely deployed around each LoRa receiver, the coverage probability of LoRa nodes will be enhanced.*

If the considered networks are *intra-interference limited*, that is, $I_{\text{inter}} = I_{\text{co}} = 0$ and $\sigma^2 = 0$, then from (30) and (31), we can obtain the following propagation.

Proposition 1. *For the unordered intra-interference limited case, the coverage probability of the case with a fixed number of active nodes n in the cluster can be expressed as*

$$P^{n,ap}_{\text{intra,up}}(\gamma_{th}) \approx \omega_M \sum_{m=1}^{M} \vartheta_m l_m \left[\omega_T \sum_{t=1}^{T} \frac{\mu_t c_t^{\alpha+1}}{c_t^{\alpha} + \gamma_{th}\tilde{P}_x^{-1}} \right]^{n-1}, \tag{33}$$

and the coverage probability of the case with a random number of active LoRa nodes in the cluster with average $\bar{n}$ can be expressed as

$$P^{\bar{n},ap}_{\text{intra,low}}(\gamma_{th}) \approx \omega_M \sum_{m=1}^{M} \vartheta_m l_m \exp\left(-(\bar{n}-1) \sum_{t=1}^{T} \frac{\omega_T \mu_t c_t}{\frac{c_t^{\alpha}\tilde{P}_x}{l_m^{\alpha}\gamma_{th}} + 1} \right). \tag{34}$$

Remark 3. *When the networks are intra-interference limited, from* (30) *and* (34)*, the coverage probability is independent of the cluster radius, a, which is intuitive.*

B. Coverage Probability of Ordered LoRa Users

Based on the derived results in Section III, we can obtain the coverage probability of the k-th closest LoRa node in the ordered case in this subsection.

The transmission coverage probability of the k-th closest LoRa node can be expressed as

$$P^{k}_{\text{cov}}(\gamma_{th}) = \int_{R^+} \Pr\{\text{SINR}(\tilde{r}_k) \geq \gamma_{th}\} f_{\tilde{r}_k}(\tilde{r}_k)\, d\tilde{r}_k, \tag{35}$$

Theorem 2. *If the LoRa nodes follow a Matern cluster process centered around each receiver, the coverage probability of the k-th closest LoRa node located in a cluster of n active LoRa nodes can be expressed as*

$$P^{n,k}_{\text{cov,up}}(\gamma_{th}) = \int_0^a e^{-\rho_k \sigma^2} L_{I^{n,k}_{\text{intra}}}(\rho_k) L^{up}_{I^{n}_{\text{inter}}}(\rho_k)\, L_{I_{\text{co}}}(\rho_k) \times \frac{2n!\tilde{r}_k^{2k-1}\left(1-\tilde{r}_k^2 a^{-2}\right)^{n-k}}{a^{2k}(n-k)!(k-1)!} d\tilde{r}_k, \tag{36}$$

where $\rho_k = \frac{\tilde{r}_k^{\alpha}\gamma_{th}}{\tilde{P}_{x_0}\eta}$, $\mathcal{L}_{I^{n,k}_{\text{intra}}}(\rho_k)$, $\mathcal{L}^{up}_{I^{n}_{\text{inter}}}(\rho)$, and $\mathcal{L}_{I_{\text{co}}}(\rho)$ are given by (19)*,* (15)*, and* (17)*.*

The coverage probability of the k-th closest LoRa node located in a cluster with a random number of active nodes with average $\bar{n}$ can be expressed as

$$P^{\bar{n},k}_{\text{cov,low}}(\gamma_{th}) = \int_0^a e^{-\rho_k \sigma^2} L_{I^{\bar{n},k}_{\text{intra}}}(\rho_k) L^{low}_{I^{\bar{n}}_{\text{inter}}}(\rho_k)\, L_{I_{\text{co}}}(\rho_k) \times \frac{2n!\tilde{r}_k^{2k-1}\left(1-\tilde{r}_k^2 a^{-2}\right)^{n-k}}{a^{2k}(n-k)!(k-1)!} d\tilde{r}_k, \tag{37}$$

where $\rho_k = \frac{\tilde{r}_k^{\alpha}\gamma_{th}}{\tilde{P}_{x_0}\eta}$, $\mathcal{L}_{I^{\bar{n},k}_{\text{intra}}}(\rho_k)$, $\mathcal{L}^{low}_{I^{\bar{n}}_{\text{inter}}}(\rho_k)$, and $\mathcal{L}_{I_{\text{co}}}(\rho_k)$ are given by (22)*,* (16)*, and* (17)*.*

Proof. By applying (7) and (1) into (35), we obtain the desired results. The proof is completed. □

Corollary 4. *If the LoRa nodes follow a Matern cluster process centered around each receiver, the coverage probability of the k-th closest LoRa node, which is located in a cluster with a fixed number of active nodes n, can be approximated as* (38)*, which is given on the next page.*

For the cluster with a random number of active LoRa nodes of average $\bar{n}$, the coverage probability of the k-th closest LoRa node can be approximated as

V. Area Spectral Efficiency and Energy Efficiency

Spectral efficiency and energy efficiency are two critical factors for the design of LPWA networks, as LPWA networks are required to support massive connectivity with minimal energy consumption at sensor nodes. We will investigate the area spectral efficiency and energy efficiency in this section.

A. Area Spectral Efficiency

The area spectral efficiency is defined as the average data in bits that all transmitters can contribute per unit area. Therefore, based on section III, we can get the area spectral efficiency in the following proposition.

Proposition 2. *The area spectral efficiency of a given network can be expressed as*

$$\tau = n_\iota \lambda_G R_t P^{ap}_{\text{cov}}, \tag{40}$$

where $R_t = \log_2(1+\gamma_{th})$ is the transmission rates of all LoRa nodes, P^{ap}_{cov} is given by (30)*,* (31)*,* (38)*, and* (39) *for the four scenarios considered in this paper, respectively.*

If the density of LoRa receivers λ_G, the density of non-LoRa receivers λ_{co}, and the number of active LoRa nodes in each cluster $n_\iota = \{n, \bar{n}\}$ are fixed, according to (40), we have the following remarks.

Remark 4. *The area spectral efficiency is a monotonically decreasing function of the cluster radius a according to* (40)*. Therefore, the area spectral efficiency can be enhanced by densely deploying LoRa nodes around each LoRa receiver.*

Remark 5. *The area spectral efficiency is not a monotonic function of the number of active LoRa nodes n_ι in the cluster according to* (40)*. Therefore, the area spectral efficiency can be maximized by adjusting the number of active LoRa nodes around each LoRa receiver properly. Due to the complex expressions of* (30)*,* (31)*,* (38)*, and* (39)*, the number of active LoRa nodes in the cluster that achieves the maximal area spectral efficiency is shown in the simulation results.*

$$P_{\mathrm{cov,up}}^{k,ap}\left(\gamma_{th}\right) \approx \omega_M \sum_{m=1}^{M} \vartheta_m \frac{n! {l_m}^{2k-1}\left(1-{l_m}^2\right)^{n-k}}{(n-k)!\,(k-1)!} \times \exp\left(-\rho_m \sigma^2\right) \left[\omega_T \sum_{t=1}^{T} \frac{\mu_t c_t^{\alpha+1}}{c_t^{\alpha}+\gamma_{th}\tilde{P}_x^{-1}}\right]^{k-1} \times \left[\frac{\omega_T}{1-{l_m}^2}\left(\sum_{t=1}^{T} \frac{\mu_t c_t^{\alpha+1}}{c_t^{\alpha}+{l_m}^{\alpha}\tilde{P}_x^{-1}\gamma_{th}} - {l_m}^2 \sum_{t=1}^{T} \frac{\mu_t c_t^{\alpha+1}}{c_t^{\alpha}+\gamma_{th}\tilde{P}_x^{-1}}\right)\right]^{n-k} \times \exp\left[-a^2 l_m^2 \pi \lambda_G \delta \sum_{p=1}^{n} \binom{n}{p} B\left(p-\delta, n-p+\delta\right)\left(\gamma_{th}\tilde{P}_x^{-1}\right)^{\delta} - \frac{a^2 l_m^2 \pi^2 \delta}{\sin\left(\pi\delta\right)} \lambda_{\mathrm{co}}\left(\gamma_{th}\tilde{P}_z^{-1}\right)^{\delta}\right]. \tag{38}$$

$$P_{\mathrm{cov,low}}^{w,app}\left(\gamma_{th}\right) \approx \omega_M \sum_{m=1}^{M} \vartheta_m \frac{\bar{n}! {l_m}^{2k-1}\left(1-{l_m}^2\right)^{\bar{n}-k}}{(\bar{n}-k)!\,(k-1)!} \times \exp\left(-\rho_m \sigma^2\right) \exp\left(-\left(\bar{n}-1\right)\omega_T \sum_{t=1}^{T} \frac{\mu_t c_t}{c_t^{\alpha}\tilde{P}_x\left(\gamma_{th}\right)^{-1}+1}\right) \times \exp\left[-\frac{a^2 l_m^2 \pi^2 \delta}{\sin\left(\pi\delta\right)}\left(\lambda_G \bar{n}\left(\gamma_{th}\tilde{P}_x^{-1}\right)^{\delta} + \lambda_{\mathrm{co}}\left(\gamma_{th}\tilde{P}_z^{-1}\right)^{\delta}\right)\right]. \tag{39}$$

B. Energy Efficiency

For a given network, the total power consumption for nodes within per unit area is $n_\iota \lambda_G P_x$, where P_x is the transmit power. Energy efficiency is defined as the ratio of the total amount of data delivered and the total energy consumed.

Proposition 3. *Based on* (40)*, we can obtain the energy efficiency of the considered network as*

$$\mathrm{EE} = \frac{n_\iota \lambda_G R_t P_{\mathrm{cov}}^{ap}}{n_\iota \lambda_G P_x} = \frac{R_t P_{\mathrm{cov}}^{ap}}{P_x}, \tag{41}$$

where R_t and P_{cov}^{ap} are same as defined in (40)*.*

Remark 6. *Energy efficiency is a monotonically decreasing function of cluster radius, a. Therefore, the energy efficiency of a given network can be enhanced by densely deploying LoRa nodes around each LoRa receiver.*

VI. Numerical Results

We first validate the analytical results presented in the earlier sections and investigate the tightness of various approximations derived for coverage probability. In our simulation, the locations of LoRa nodes are drawn from a PCP over a circle region with radius $R_n = 20$ km as LoRa claims that it is able to support long range transmission in terms of kilometers. The simulation parameters are set according to the LoRa specifications unless stated otherwise. The transmission frequency is $f_c = 868$ MHz as it is used for LoRa in Europe [15]. The bandwidth is $BW = 125$ KHz as one of most common setting-ups for LoRa networks. The thermal noise in dBm level is calculated as $\sigma^2 = -174 + 10\log_{10}\left(BW\right)$. The path-loss exponent for the communication links is $\alpha = 3.5$. For the ordered case, we take $k = \mathcal{N}$ to show the achievable performance of the LoRa node that locates farthest away from the LoRa receiver.

Fig. 2 plots the coverage probability of the networks with different SINR thresholds at the receivers γ_{th}. We can see that the derived closed-form expressions in Corollaries 3 and 4 are well matched with Theorems 1 and 2. Therefore, we use the approximations given in Corollaries 3 and 4 as the analytical results in the following figures. It is also worth noting that the unordered case always achieves better coverage probability than the ordered case. The reason is that in the ordered case the farthest LoRa node is chosen as the the typical one by taking $k = \mathcal{N}$. For the unordered case, the LoRa node of interest is selected randomly among the active nodes in the same cluster, which results in an average performance of the considered networks.

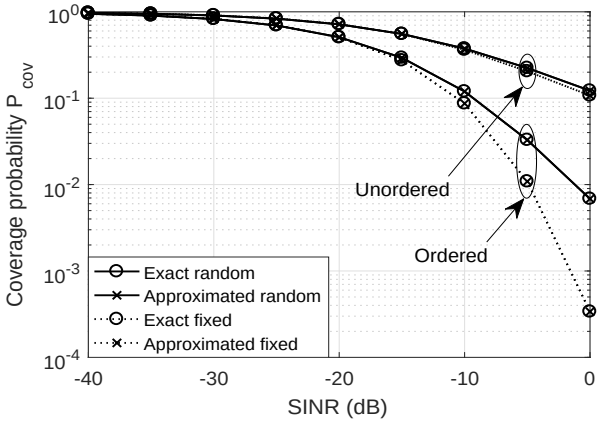

Fig. 2. Verification of exact and approximated results versus SINR thresholds γ_{th}, transmit power is $P_x = 14$ dBm, and density of LoRa receivers and coexisted non-LoRa nodes are $\lambda_G = \lambda_{\mathrm{co}} = 10^{-1}/\left(500^2\pi\right)$, cluster radius is $a = 500$ m, and the number of active LoRa nodes in the cluster is $n_\iota = 6$.

Fig. 3 plots the coverage probability of the networks for the ordered and unordered cases versus the number of active LoRa nodes in each cluster n_ι. For the curve, we can observe the following:

1) The coverage probability decreases with larger cluster radius a, which is consistent with the discussion in Remark 2. This is due to the fact that larger a not only increases the distance of the desired link but also the inter-cluster interference, because larger a shortens the distance between sources of inter-cluster interference and the typical receiver.

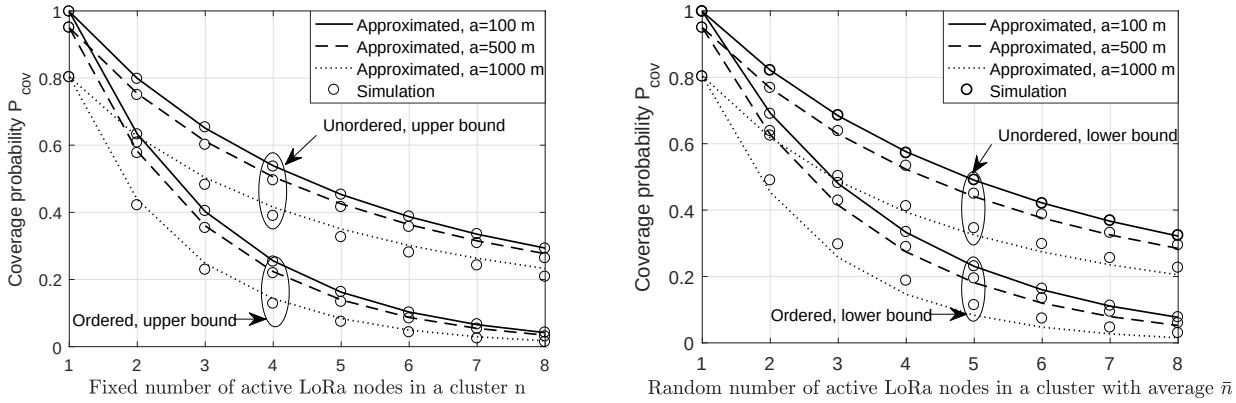

(a) (b)

Fig. 3. Verification of approximated and simulation results versus number of active LoRa nodes in each cluster with different cluster radii a, density of LoRa receivers and non-LoRa nodes are $\lambda_G = \lambda_{\rm co} = 10^{-1}/\left(500^2\pi\right)$, transmit power is $P_x = 14$ dBm, SINR threshold is $\gamma_{th} = -10$ dB.

2) It is also worth noting that the approximated results given in (30), (31), (38) and (39) are well matched with the simulation results when the cluster radius is $a = 100$ m. With increasing a, there is a small but notable gap between the approximated results and the simulation results, which is caused by using the distance approximation, $q\left(x, y, \theta\right) \approx y$, in Section III. In a practical scenario of LPWA networks, the cluster radius a is typically a value in terms of kilometers. Here, we provide results with $a = 100$ m is just to justify the tightness of our derived approximated results.

As observed from Fig. 2 and Fig. 3, the unordered case behaves similarly to the ordered case. In order to save space without losing any important insights, in the following figures, we only present the results of the ordered case with a fixed and a random number of active LoRa nodes, respectively.

Fig. 4 plots the coverage probability of the networks for ordered cases versus density of active LoRa nodes $n_\iota \lambda_G$ with different densities of non-LoRa nodes $\lambda_{\rm co}$. Both the cases with fixed and random numbers of active LoRa nodes in each cluster are presented. It is worth noting that coverage probability is monotonically decreasing with density of active LoRa nodes $n_\iota \lambda_G$ and the density of non-LoRa nodes $\lambda_{\rm co}$. The reason is that larger densities of active LoRa nodes and non-LoRa nodes bring higher intra-interference, inter-interference, and coexistence interference. This phenomenon is consistent with the discussion in Remark 1.

Fig. 5 plots the area spectral efficiency of the networks versus the number of active LoRa nodes n_ι simultaneously transmitting in each cluster with different cluster radii a. From the curve, the area spectral efficiency is monotonically decreasing with the cluster radius a, which is consistent with the discussion in Remark 4. We can also observe that the area spectral efficiency is not a monotonic function of n_ι as discussed in Remark 5. In other words, there exists an optimal number of active LoRa links. This behavior can be explained as follows: on the one hand, more simultaneously transmitting LoRa links bing larger intra-cluster interference, as such, the coverage probability decreases, which in turn decreases the area spectral efficiency. On the other hand, as seen from (40), larger n_ι results in more efficient spectrum unitization per unit area, which enhances the area spectral efficiency.

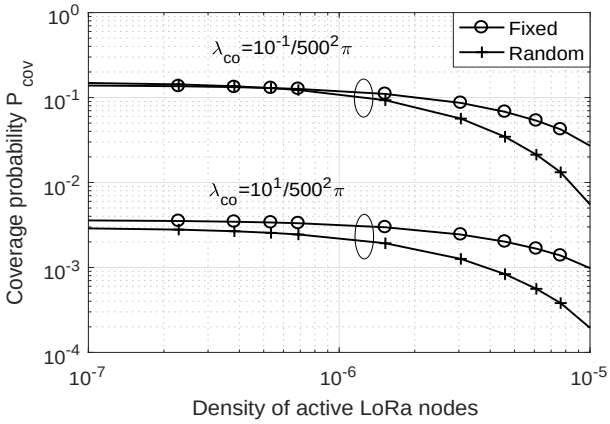

Fig. 4. Coverage probability versus density of ordered active LoRa nodes with different density of non-LoRa nodes $\lambda_{\rm co}$, transmit power is $P_x = 14$ dBm, SINR threshold is $\gamma_{th} = -10$ dB, cluster radius is $a = 500$ m, number of active LoRa nodes in the cluster is $n_\iota = 6$.

Fig. 6 plots the energy efficiency of the networks versus the cluster radius a with different transmit powers P_x. We can see that the energy efficiency is monotonically decreasing with the cluster radius a, which is consistent with the discussion in Remark 6. We also observe that the energy efficiency is not a monotonically decreasing function with the transmit power P_x according to (41). However, when the transmit power is set to 0 dBm, 7 dBm and 14 dBm as specified in LoRa networks, the energy efficiency decreases monotonically.

Fig. 7 verifies the necessity of considering noise in the analysis by comparing the coverage probability for cases with and without noise. It can be shown that the coverage probability of the interference-limited case is always higher than that with both interference and noise. This is mainly because that the distance from LoRa users to gateway is usually very long with low transmit power in LPWA networks.

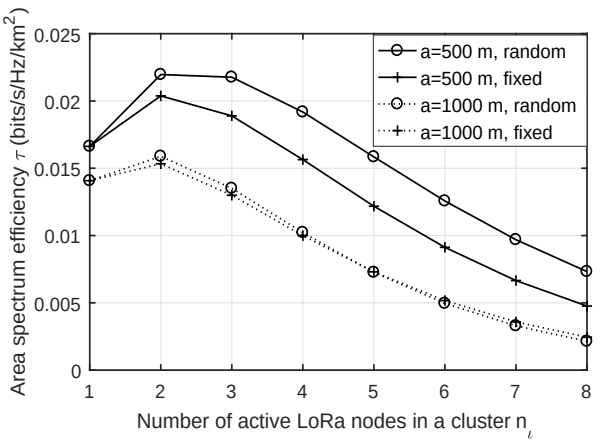

Fig. 5. Area spectral efficiency versus the number of ordered active LoRa nodes in each cluster for ordered and unordered cases with different cluster radii a, density of LoRa receivers and non-LoRa nodes are $\lambda_G = \lambda_{\rm co} = 10^{-1}/\left(500^2\pi\right)$, transmit power is $P_x = 14$ dBm, and SINR threshold is $\gamma_{th} = -10$ dB.

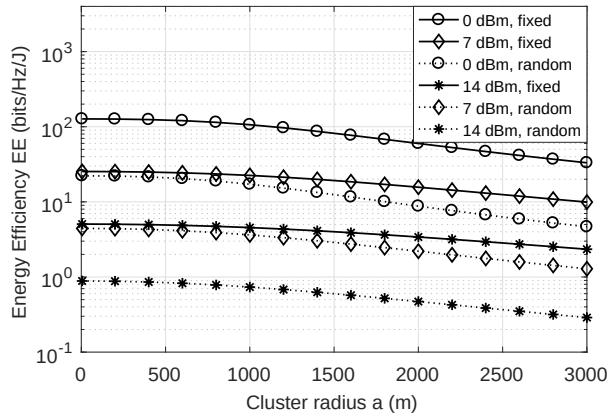

Fig. 6. Energy efficiency versus cluster radius a with different transmit powers P_x, density of LoRa receivers and non-LoRa nodes are $\lambda_G = \lambda_{\rm co} = 10^{-1}/\left(500^2\pi\right)$, and SINR threshold is $\gamma_{th} = -10$ dB.

As part of a smart city project, the above observations are capable of providing insights when determining the system parameters of LoRa networks in practical scenarios. For example, with the purpose of maximizing the area spectral efficiency of an LPWA network, there exists an optimal number of LoRa nodes transmitting to the the LoRa receiver simultaneously. This inspires the strategy for when and how to scale the LoRa network by introducing new LoRa gateways in order to achieve the optimal area spectral efficiency. Another example is that in order to improve the energy efficiency of an LPWA network, transmit power should be minimized if the LoRa node is within the coverage of a LoRa receiver.

VII. Conclusions

In this paper, the uplink transmission of low-power wide-area (LPWA) networks with multiple radio modules has been studied. By using LoRa as an application of our technique and accounting for coexistence interference from other types of radio modules sharing the space, we investigated the performance of the LPWA networks with invoking the poisson cluster process (PCP) to model the locations of LoRa nodes. Specifically, we consider the scenarios that the number of active LoRa nodes in each cluster is fixed and random, respectively, and that the typical LoRa node is chosen randomly or according to the distance from the typical node to its serving receiver. Besides the exact expressions, we have also derived the simple and approximated expressions for the coverage probability of a typical LoRa node, its area spectral efficiency, and its energy efficiency. According to our analyses, an effective approach for enhancing network performance is to deploy nodes more densely but there exists an optimal number of active LoRa nodes in each cluster to maximize the area spectral efficiency. Furthermore, energy efficiency decreases monotonically with the transmit power using the values that are specified in LoRa specification. As part of a smart city project, our results here can provide insightful guidelines to inform our real world deployment of the large-scale LPWA networks.

VIII. Acknowledgement

The authors would like to thank Dr. Mo Haghighi from Intel Labs Europe for his clarification regarding the specifics & LoRa protocol.

Appendix A: Proof of Lemma 3

For the unordered case with n active LoRa nodes in each cluster, the Laplace transforms of intr-cluster interference is given by

$$\begin{aligned}
\mathcal{L}_{I^n_{\rm intra}}(s) &= \mathbb{E}_{x\in N_{y_0}\setminus x_0}\left[\exp\left(-s\sum_{x\in N\setminus x_0} P_x h_{x,y_0}\eta\|x\|^{-\alpha}\right)\right] \\
&= \mathbb{E}_{x\in N_{y_0}\setminus x_0}\left[\prod_{x\in N_{y_0}} \mathbb{E}_{h_{x,y_0}}\left[\exp\left(-sP_x h_{x,y_0}\eta\|x\|^{-\alpha}\right)\right]\right] \\
&\overset{(a)}{=} \mathbb{E}_{x\in N_{y_0}\setminus x_0}\left[\prod_{x\in N_{y_0}\setminus x_0} \frac{1}{1+sP_x\eta\|x\|^{-\alpha}}\right] \\
&= \left[\int_R \left(\frac{1}{1+sP_x\eta\|x\|^{-\alpha}}\right) f_{\|x\|}(x)\,dx\right]^{n-1} \\
&\overset{(b)}{=} \left[\int_0^a \left(\frac{1}{1+sP_x\eta r^{-\alpha}}\right) f_R(r)\,dr\right]^{n-1}, \qquad \text{(A.1)}
\end{aligned}$$

where (a) follows the fact that h_{x,y_0} follows a Rayleigh fading distribution with unit mean, (b) is obtained by changing the integration from the Cartesian coordinates into the polar coordinates. Plugging (6) into (A.1) and letting $t = r^\alpha$, we can obtain

$$\mathcal{L}_{I^n_{\rm intra}}(s) = \left[\frac{\delta}{a^2 sP_x\eta}\int_0^{a^\alpha}\left(\frac{t^\delta}{t(sP_x\eta)^{-1}+1}\right)dt\right]^{n-1}. \qquad \text{(A.2)}$$

Then applying [41, Eq. (3.194).1], we can obtain (11).

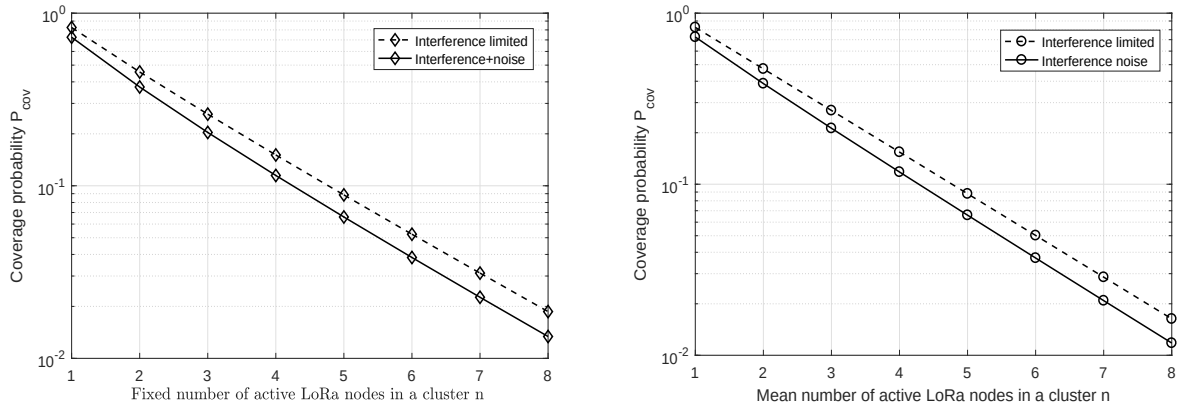

(a) (b)

Fig. 7. Coverage probability versus the number of active LoRa nodes in each cluster, density of LoRa receivers and non-LoRa nodes are $\lambda_G = \lambda_{\rm co} = 10^{-1}/\left(500^2\pi\right)$, cluster radius is $a = 1000$ m, transmit power is $P_x = 7$ dBm, SINR threshold is $\gamma_{th} = -10$ dB.

Following the similar procedure of obtaining (11), we have

$$\mathcal{L}_{I^{\bar{n}}_{\rm intra}}(s) \overset{(a)}{=} \mathbb{E}_{x\in N_{y_0}\setminus x_0}\left[\prod_{x\in N_{y_0}\setminus x_0}\frac{1}{1+sP_x\eta\|x\|^{-\alpha}}\right]$$
$$\overset{(b)}{=} \exp\left[(\bar{n}-1)\int_{R^+}\left(1-\frac{1}{1+sP_x\eta\|x\|^{-\alpha}}\right)f_{\|x\|}(x)\,dx\right], \tag{A.3}$$

where (a) follows the fact that h_{x,y_0} follows a Rayleigh fading distribution with unit mean, (b) is obtained by applying the moment-generating function. Substituting (5) into (A.3) and changing the integration from the Cartesian coordinates into the polar, we have

$$\mathcal{L}_{I^{\bar{n}}_{\rm intra}}(s) = \exp\left(-\frac{2(\bar{n}-1)}{a^2}\int_0^a \frac{sP_x\eta r^{-\alpha}}{1+sP_x\eta r^{-\alpha}} r dr\right). \tag{A.4}$$

With the aid of [41, Eq. (3.194).1], we obtain (12). The proof is completed.

Appendix B: Proof of (15) in Lemma 4

Based on (3), the the Laplace transform for inter-cluster interference with n active LoRa nodes in the cluster is given by

$$\mathcal{L}_{I^{n}_{\rm inter}}(s)$$
$$= \mathbb{E}_{\Phi_G}\left[\prod_{y\in\Phi_G\setminus y_0}\exp\left(-s\sum_{x\in N_y}P_x h_{x,y}\eta\|y+x\|^{-\alpha}\right)\right]$$
$$\overset{(a)}{=} \mathbb{E}_{\Phi_G}\left[\prod_{y\in\Phi_G\setminus y_0}\mathbb{E}_x\left[\prod_{x\in N_y}\left(\frac{1}{1+sP_x\eta\|y+x\|^{-\alpha}}\right)\right]\right]$$
$$\overset{(b)}{=} \exp\left[-\lambda_G\times\right.$$
$$\left.\int_{R^2}\left(1-\left[E_x\left(\frac{1}{\left(1+sP_x\eta\|y+x\|^{-\alpha}\right)^n}\right)\right]^n\right)dy\right], \tag{B.1}$$

where (a) is obtained by $h_{x,y}$ follows the Rayleigh distribution with unit mean, (b) is obtained with using the generating functional of *Matern* point process with a fixed number of points n in each cluster. With the aid of Jensen inequality $\left[\mathbb{E}_x(x)\right]^n \le \mathbb{E}_x\left((x)^n\right)$, we can obtain a tight upper bound for the Laplace transform of inter-cluster interference, which is given by

$$\mathcal{L}_{I^{n}_{\rm inter}}(s) \le \mathcal{L}^{up}_{I^{n}_{\rm inter}}(s)$$
$$\overset{(a)}{=} \exp\left[-\lambda_G\int_{R^2} f_{\|x\|}(x)\,dx\right)$$
$$\times\left(\int_{R^2}\left[1-\frac{1}{\left(1+sP_x\eta\|y^*\|^{-\alpha}\right)^n}\right]dy^*\right)\Bigg]$$
$$\overset{(b)}{=} \exp\left(-2\pi\lambda_G\int_0^\infty\left(1-\frac{1}{(1+sP_x\eta r^{-\alpha})^n}\right)r dr\right)$$
$$\overset{(c)}{=} \exp\left(-2\pi\lambda_G\sum_{p=1}^{n}\binom{n}{p}(sP_x\eta)^p\int_0^\infty\frac{r^{-\alpha p+1}}{(1+sP_x\eta r^{-\alpha})^n}dr\right)$$
$$\overset{(d)}{=} \exp\left(-\pi\lambda_G\sum_{p=1}^{n}\binom{n}{p}(sP_x\eta)^\delta\delta\int_0^\infty\frac{(t)^{p-\delta-1}}{(1+t)^n}dt\right)$$
$$\overset{(e)}{=} \exp\left(-\pi\lambda_G(sP_x\eta)^\delta\delta\sum_{p=1}^{n}\binom{n}{p}B(p-\delta,n-p+\delta)\right), \tag{B.2}$$

where (a) is obtained by changing variables as $y^* \to y+x$, (b) is obtained by changing from cartesian to polar coordinate, (c) is obtained by applying Binomial expansion, (d) is resulted from using the variable changes of $t = \frac{sP_x\eta}{r^\alpha}$, and (e) is simplified with applying the definition of Beta function [41, Eq. (8.380) .3].

Appendix C: Proof of (16) in Lemma 4

Similar to (B.2), the the Laplace transform for inter-cluster interference with a random number of active LoRa nodes in

the cluster with an average $\bar{n}$ is written by

$$\mathcal{L}_{I^{\bar{n}}_{\text{inter}}}(s) = \mathbb{E}_{\Phi_G}\left[\prod_{y\in\Phi_G\setminus y_0}\mathbb{E}_x\left[\prod_{x\in N_y}\left(\frac{1}{1+sP_x\eta\|y+x\|^{-\alpha}}\right)\right]\right]. \tag{C.1}$$

Applying the the generating functional of *Matern* point process with a random number of points of average $\bar{n}$, and similar to (B.2) with the variables changes of $y^* \to y+x$, we can obtain

$$\begin{aligned}\mathcal{L}_{I^{\bar{n}}_{\text{inter}}}(s) &= \exp\left(-\lambda_G\int_{R^2}\left(1-\exp\left(-\bar{n}\left(\frac{sP_x\eta y^{*-\alpha}}{1+sP_x\eta y^{*-\alpha}}\right)\right)\right)dy^*\right)\\ &= \exp\left(-2\pi\lambda_G\int_0^\infty\left[1-\exp\left(-\bar{n}\left(\frac{sP_x\eta r^{-\alpha}}{1+sP_x\eta r^{-\alpha}}\right)\right)\right]rdr\right)\end{aligned} \tag{C.2}$$

With the aid of Taylor series expansion, we can have the approximation as $1-\exp(-x)\le x$. Then we can obtain

$$\begin{aligned}\mathcal{L}_{I^{\bar{n}}_{\text{inter}}}(s) &\ge \mathcal{L}^{low}_{I^{\bar{n}}_{\text{inter}}}(s)\\ &= \exp\left(-2\pi\lambda_G\bar{n}\int_0^\infty\left(\frac{sP_x\eta r^{-\alpha}}{1+sP_x\eta r^{-\alpha}}\right)rdr\right)\\ &\overset{(a)}{=} \exp\left(-\pi\lambda_G\bar{n}(sP_x\eta)^\delta\delta\Gamma(\delta)\Gamma(1-\delta)\right)\\ &\overset{(b)}{=} \exp\left(-\pi^2\lambda_G\bar{n}(sP_x\eta)^\delta\frac{\delta}{\sin(\pi\delta)}\right),\end{aligned} \tag{C.3}$$

where (a) is obtained by applying [41, Eq. (3.241).4], and (b) is obtained with the aid of the Euler's reflection formula. The proof is completed.

Appendix D: Proof of Lemma 6

The Laplace transform of intra-cluster interference can be divided into two disjoint sets, as mentioned in Section III. By doing so, the Laplace transform of intra-cluster interference for the case with n active LoRa nodes in the cluster can be expressed as

$$\begin{aligned}\mathcal{L}_{I^{n,k}_{\text{intra}}}(s) &= \mathbb{E}\left[\prod_{x\in K_{near}}\frac{1}{1+sP_x\eta\|x\|^{-\alpha}}\prod_{x\in K_{far}}\frac{1}{1+sP_x\eta\|x\|^{-\alpha}}\right]\\ &\overset{(a)}{=}\left[\int_{R^+}\left(\frac{1}{1+sP_x\eta r^{-\alpha}}\right)f_{\tilde{R}|r\le\tilde{r}_k}(r|\,\tilde{r}_k)\,dr\right]^{k-1}\\ &\times\left[\int_{R^+}\left(1-\frac{1}{1+sP_x\eta r^{-\alpha}}\right)f_{\tilde{R}|r>\tilde{r}_k}(r|\,\tilde{r}_k)\,dr\right]^{n-k}\\ &\overset{(b)}{=}\left[\frac{2}{\tilde{r}_k^2}\underbrace{\int_0^{\tilde{r}_k}\left(\frac{1}{1+sP_x\eta r^{-\alpha}}\right)rdr}_{Q_1}\right]^{k-1}\\ &\times\left[\frac{2}{a^2-\tilde{r}_k^2}\underbrace{\int_{\tilde{r}_k}^{a}\left(\frac{1}{1+sP_x\eta r^{-\alpha}}\right)rdr}_{Q_2}\right]^{n-k},\end{aligned} \tag{D.1}$$

where (a) is obtained by applying generating functional of *Matern* point process with fixed number of points n, (b) is obtained by plugging (10) inside, which is PDF of the ordered distance for intra-cluster interference nodes.

Using the similar approach as obtaining (A.2), we can obtain

$$Q_1 = \frac{\delta}{2sP_x\eta}\frac{\tilde{r}_k^{\alpha+2}}{\delta+1}{}_2F_1\left(1,\delta+1;\delta+2;-\frac{\tilde{r}_k^\alpha}{sP_x\eta}\right) \tag{D.2}$$

and

$$\begin{aligned}Q_2 =& \frac{\delta}{2sP_x\eta}\frac{a^{\alpha+2}}{\delta+1}F_1\left(1,\delta+1;\delta+2;-\frac{a^\alpha}{sP_x\eta}\right)\\ &-\frac{\delta}{2sP_x\eta}\frac{\tilde{r}_k^{\alpha+2}}{\delta+1}F_1\left(1,\delta+1;\delta+2;-\frac{\tilde{r}_k^\alpha}{sP_x\eta}\right),\end{aligned} \tag{D.3}$$

respectively. Substituting into (D.2) and (D.3) into (D.1), we can obtain (19).

The proof of (22) follows on the same procedure as (19) and is hence skipped.

References

[1] Z. Qin, Y. Liu, G. Y. Li, and J. A. McCann, "Modelling and analysis of low-power wide-area networks," in *Proc. Int. Commun. Conf. (ICC'17)*, Paris, France, May 2017, pp. 1–7.

[2] J. Kim, J. Yun, S. C. Choi, D. N. Seed, G. Lu, M. Bauer, A. Al-Hezmi, K. Campowsky, and J. Song, "Standard-based IoT platforms interworking: implementation, experiences, and lessons learned," *IEEE Wireless Commun.*, vol. 54, no. 7, pp. 48–54, July 2016.

[3] G. Xie, K. Ota, M. Dong, F. Pan, and A. Liu, "Energy-efficient routing for mobile data collectors in wireless sensor networks with obstacles," *Peer-to-Peer Netw. App.*, vol. 10, no. 3, pp. 472–483, May 2017.

[4] Z. Qin, J. Fan, Y. Liu, Y. Gao, and G. Y. Li, "Sparse representation for wireless communications: A compressive sensing approach," *IEEE Signal Process. Mag.*, vol. 35, no. 3, pp. 40–58, May 2018.

[5] M. Tao, K. Ota, and M. Dong, "Locating compromised data sources in IoT-enabled smart cities: A great-alternative-region-based approach," *IEEE Trans. Industr. Info.*, vol. 14, no. 6, pp. 2579–2587, Jun. 2018.

[6] Z. Qin, H. Ye, G. Y. Li, and B. F. Juang, "Deep learning in physical layer communications," *IEEE Wireless Commun.*, vol. 26, no. 2, pp. 93–99, Apr. 2019.

[7] S. K. Sharma and X. Wang, "Towards massive machine type communications in ultra-dense cellular IoT networks: Current issues and machine learning-assisted solutions," *arXiv preprint arXiv:1808.02924*, 2018.

[8] H. Li, K. Ota, and M. Dong, "Eccn: Orchestration of edge-centric computing and content-centric networking in the 5G radio access network," *IEEE Wireless Commun.*, vol. 25, no. 3, pp. 88–93, Jun. 2018.

[9] X. Xiong, K. Zheng, R. Xu, W. Xiang, and P. Chatzimisios, "Low power wide area machine-to-machine networks: key techniques and prototype," *IEEE Commun. Mag.*, vol. 53, no. 9, pp. 64–71, Sep. 2015.

[10] M. R. Palattella, M. Dohler, A. Grieco, G. Rizzo, J. Torsner, T. Engel, and L. Ladid, "Internet of Things in the 5G era: Enablers, architecture, and business models," *IEEE J. Sel. Areas Commun.*, vol. 34, no. 3, pp. 510–527, Mar. 2016.

[11] M. Centenaro, L. Vangelista, A. Zanella, and M. Zorzi, "Long-range communications in unlicensed bands: the rising stars in the IoT and smart city scenarios," *IEEE Wireless Commun.*, vol. 23, no. 5, pp. 60–67, Oct. 2016.

[12] Z. Qin, F. Y. Li, G. Y. Li, J. A. McCann, and Q. Ni, "Low-power wide-area networks for sustainable IoT," *IEEE Wireless Commun.*, Jan. 2019.

[13] "LPWAN technology decisions." [Online]. Available: http://www.weightless.org/membership/lpwan-technology-features-document-update

[14] "Sigfox", accessed Oct. 2016. [Online]. Available: https://www.sigfox.com/

[15] N. Sornin, M. Luis, T. Eirich, T. Kramp, and O.Hersent, "LoRaWAN specification," Jan. 2015. [Online]. Available: https://www.lora-alliance.org/portals/0/specs/LoRaWAN%20Specification%201R0.pdf

[16] O. Georgiou and U. Raza, "Low power wide area network analysis: Can LoRa scale?" *IEEE Wireless Commun. Lett.*, vol. 6, no. 2, pp. 162–165, Apr. 2017.

[17] M. Bor, J. Vidler, and U. Roedig, "LoRa for the Internet of Things," in *Proc. Intl. Conf. Embedded Wireless Systems Netw., (EWSN'16)*, Feb. 2016, pp. 361–366.

[18] M. C. Bor, U. Roedig, T. Voigt, and J. M. Alonso, "Do LoRa low-power wide-area networks scale?" in *Proc. Intl. Conf. Modeling Analysis Simul. Wireless Mobile Syst., (MSWiM'16)*, Nov. 2016, pp. 59–67.

[19] X. Deng, G. Li, M. Dong, and K. Ota, "Finding overlapping communities based on Markov chain and link clustering," *Peer-to-Peer Netw. App.*, vol. 10, no. 2, pp. 411–420, Mar. 2017.

[20] T. Voigt, M. Bor, U. Roedig, and J. Alonso, "Mitigating inter-network interference in LoRa networks," in *Proc. Int. Conf. Embedded Wireless Systems Netw. (EWSN'17)*, Uppsala, Sweden, Feb. 2017, pp. 323–328.

[21] A. Froytlog, T. Foss, O. Bakker, G. Jevne, M. A. Haglund, F. Y. Li, J. Oller, and G. Y. Li, "Ultra-low power wake-up radio for 5G IoT," *IEEE Commun. Mag.*, vol. 57, no. 3, pp. 111–117, Mar. 2019.

[22] Z. Qin and J. A. McCann, "Resource efficiency in low-power wide-area networks for IoT applications," in *Proc. IEEE Global Commun. Conf. (GLOBECOM'17)*, Singapore, Dec. 2017, pp. 1–7.

[23] B. Su, Z. Qin, and Q. Ni, "Energy efficient resource allocation for uplink lora networks," in *Proc. IEEE Global Commun. Conf. (GLOBECOM'18)*, Abu Dhabi, UAE, Dec. 2018, pp. 1–7.

[24] M. Haenggi, J. G. Andrews, F. Baccelli, O. Dousse, and M. Franceschetti, "Stochastic geometry and random graphs for the analysis and design of wireless networks," *IEEE J. Sel. Areas Commun.*, vol. 27, no. 7, pp. 1029–1046, Sept. 2009.

[25] R. K. Ganti and M. Haenggi, "Interference and outage in clustered wireless Ad Hoc networks," *IEEE Trans. Inf. Theory*, vol. 55, no. 9, pp. 4067–4086, Sept. 2009.

[26] K. Gulati, B. L. Evans, J. G. Andrews, and K. R. Tinsley, "Statistics of co-channel interference in a field of Poisson and Poisson-Poisson clustered interferers," *IEEE Trans. Signal Process.*, vol. 58, no. 12, pp. 6207–6222, Dec. 2010.

[27] B. Nosrat-Makouei, R. K. Ganti, J. G. Andrews, and R. W. Heath, "MIMO interference alignment in random access networks," *IEEE Trans. Commun.*, vol. 61, no. 12, pp. 5042–5055, Dec. 2013.

[28] Y. J. Chun, M. O. Hasna, and A. Ghrayeb, "Modeling heterogeneous cellular networks interference using poisson cluster processes," *IEEE J. Sel. Areas Commun.*, vol. 33, no. 10, pp. 2182–2195, Oct. 2015.

[29] V. Suryaprakash, J. Møller, and G. Fettweis, "On the modeling and analysis of heterogeneous radio access networks using a Poisson cluster process," *IEEE Trans. Wireless Commun.*, vol. 14, no. 2, pp. 1035–1047, Feb. 2015.

[30] K. Han and K. Huang, "Wirelessly powered backscatter communication networks: Modeling, coverage, and capacity," *IEEE Trans. Wireless Commun.*, vol. 16, no. 4, pp. 2548–2561, Apr. 2017.

[31] M. Afshang, H. S. Dhillon, and P. H. J. Chong, "Modeling and performance analysis of clustered device-to-device networks," *IEEE Trans. Wireless Commun.*, vol. 15, no. 7, pp. 4957–4972, Jul. 2016.

[32] J. Tang, G. Chen, J. P. Coon, and D. E. Simmons, "Distance distributions for Matern cluster processes with application to network performance analysis," in *Proc. IEEE Int. Conf. Commun. (ICC'17)*, Paris, France, May 2017, pp. 1–6.

[33] J. Tang, G. Chen, and J. P. Coon, "Joint coverage enhancement by power allocation in poisson clustered out-of-band D2D networks," *IEEE Trans. Veh. Technol.*, vol. 67, no. 12, pp. 11 537–11 548, Dec. 2018.

[34] D. P. Kroese and Z. I. Botev, "Spatial process generation," 2012.

[35] H. A. David and N. Nagaraja, *Order Statistics*, 3rd ed. John Wiley, 2003.

[36] E. Hildebrand, "Introduction to numerical analysis," *NewYork, NY, USA: Dover,*, 1987.

[37] Z. Ding, Z. Yang, P. Fan, and H. V. Poor, "On the performance of non-orthogonal multiple access in 5G systems with randomly deployed users," *IEEE Signal Process. Lett.*, vol. 21, no. 12, pp. 1501–1505, Dec. 2014.

[38] Y. Liu, Z. Ding, M. Elkashlan, and H. V. Poor, "Cooperative non-orthogonal multiple access with simultaneous wireless information and power transfer," *IEEE J. Sel. Areas Commun.*, vol. 34, no. 4, pp. 938–953, Apr. 2016.

[39] L. Lv, Q. Ni, Z. Ding, and J. Chen, "Application of non-orthogonal multiple access in cooperative spectrum-sharing networks over Nakagami-m fading channels," *IEEE Trans. Veh. Technol.*, vol. 66, no. 6, pp. 5506–5511, Jun. 2017.

[40] Y. Liu, Z. Qin, M. Elkashlan, Y. Gao, and L. Hanzo, "Enhancing the physical layer security of non-orthogonal multiple access in large-scale networks," *IEEE Trans. Wireless Commun.*, vol. 16, no. 3, pp. 1656–1672, Mar. 2017.

[41] I. S. Gradshteyn and I. M. Ryzhik, *Table of Integrals, Series and Products*, 6th ed. New York, NY, USA: Academic Press, 2000.